

AD693249

Ballistic Research Laboratories

TECHNICAL NOTE NO. 11

30 JUNE 1949

Supersonic Wind Tunnel Tests of Small Caliber Projectiles: Cal. .50 API M23; Cal. .60 API T39; and 20mm HEI M97 (Project TB3-0108F)

This document has been approved for public release
and sale; its distribution is unlimited.

The Ballistic Research Laboratories Technical Note is designed for use with-
in the laboratories or for issuing available information, when the occasion
demands speed.

The contents of this paper are of the nature of advance information and may
be extended or otherwise revised.

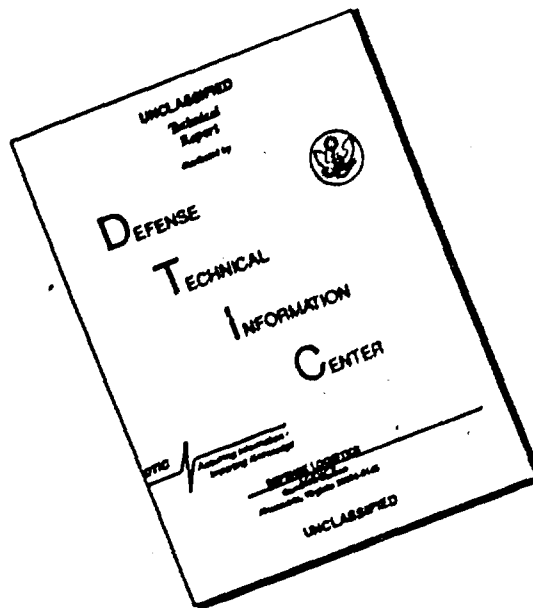
SEP 22 1969

This document contains information affecting the national defense of
the United States within the meaning of the Espionage Act, 50 U.S.C.,
31 and 32, as amended. Its transmission or the revelation of its
contents in any manner to an unauthorized person is prohibited by law.

ABERDEEN PROVING GROUND, MARYLAND

Reproduced by the
CLEARINGHOUSE
for Federal Scientific & Technical
Information Springfield Va 22151

DISCLAIMER NOTICE



THIS DOCUMENT IS BEST QUALITY AVAILABLE. THE COPY FURNISHED TO DTIC CONTAINED A SIGNIFICANT NUMBER OF PAGES WHICH DO NOT REPRODUCE LEGIBLY.


RHKrieger/aml

ABSTRACT

Three component tests of models of small caliber projectiles (Cal. .50, Cal. .60, and 20mm) were conducted in the Aberdeen Wind Tunnels at a Mach Number of 1.72 to provide aerodynamic data at high angles of attack. These results are to be used for computing the forces and motion imparted to a projectile when fired from high-speed aircraft. All projectiles were aerodynamically unstable. The addition of rifling increased the fore drag coefficient with little effect on lift and moment curve slopes. The test results are presented in graphs of aerodynamic coefficients as a function of angles of attack.

↖

This document has been approved for public release
and sale; its distribution is unlimited.

TABLE OF CONTENTS

	<u>Page</u>
Introduction	3
Definition of Symbols	3
Apparatus	4
Models	4
Test Procedure	5
Results	5
Discussion	6
Conclusions	9

INTRODUCTION

This report presents the results of tests on three small caliber projectiles (Cal. .50, Cal. .60, and 20mm) in the Aberdeen Supersonic Wind Tunnels at the request of the Office of the Chief of Ordnance. These tests were conducted to determine the stability characteristics at large angles of attack for the small projectiles. The results of these tests are to be used to calculate the motion of small projectiles fired from moving aircraft. Although the projectiles are spin stabilized in flight, the tests were made without spin, and the results must be interpreted with this condition in mind. The effect of rifling on the two small caliber projectiles (.50 and .60) was determined. These tests were performed at Mach Number 1.72 during the period between 25 November 1947 and 1 December 1947.

DEFINITION OF SYMBOLS

P_o = Supply pressure

$$P_{TS} = \text{Test section static pressure} = \frac{P_o}{\left[1 + \frac{\gamma - 1}{2} Ma^2 \right]^{\gamma / (\gamma - 1)}}$$

P_{mb} = Pressure on model base

$$q = \frac{1}{2} \rho v^2 = \frac{\gamma P_{TS} Ma^2}{2}$$

L = Lift force

N = Normal force

D_T = Total indicated drag

m = Pitching moment about the center of gravity

$$C_L = \text{Lift force coefficient} = \frac{L}{qA}$$

$$C_N = \text{Normal force coefficient} = \frac{N}{qA}$$

$$C_{D_T} = \text{Total indicated drag coefficient} = \frac{D_T}{qA}$$

$$C_{D_B} = \text{Base drag coefficient} = \frac{(P_{TS} - P_{mb})A_b}{qA}$$

$$C_{D_F} = \text{Fore drag coefficient} = C_{D_T} - C_{D_B}$$

$$C_m = \text{Pitching moment coefficient} = \frac{m}{qA}$$

$$Re = \text{Reynolds Number} = \frac{\rho V d}{\mu}$$

$$\rho = \text{Air density}$$

$$\mu = \text{Viscosity}$$

$$V = \text{Velocity}$$

$$Ma = \text{Mach Number}$$

$$\gamma = \text{Ratio of specific heats} = 1.405$$

$$A = \text{Model frontal area} = \frac{\pi}{4} d^2$$

$$d = \text{Maximum body diameter}$$

$$A_b = \text{Model base area} = \frac{\pi}{4} d_b^2$$

$$d_b = \text{Diameter of base}$$

APPARATUS

The tests reported in this Technical Note were performed in the Bomb Tunnel of the Ballistic Research Laboratories, Aberdeen Proving Ground. This tunnel is a continuous operation, closed throat, variable density, supersonic wind tunnel with a 15 by 20 inch rectangular test section.


The tunnel is equipped with a three-component hydraulic balance system with the following characteristics:

<u>Component</u>	<u>High Scale</u>		<u>Low Scale</u>	
	<u>Capacity</u>	<u>Least Count</u>	<u>Capacity</u>	<u>Least Count</u>
Lift:	+100 to -100 lb	0.2 lb	+25 to -25 lb	.05 lb
Drag	0 to 100 lb	0.1 lb	0 to 20 lb	.02 lb
Moment	+800 to -800 in-lbs	2.0 in-lbs	+200 to -200 in-lbs	0.5 in-lb

MODELS

Figures 1, 2, and 3 show the principal dimensions of the model

7



configurations tested. The models were equipped with offset struts because of the limitations of the balance range in angle of attack. All the models tested were two inches in diameter. Figures 4 and 5 show section views of the axial and offset strut installations with the alternate bases. Figures 6 through 14 are photographs of the various models and their component parts, as well as the support strut and strut fairings. The models were constructed of aluminum, the strut was made of steel, and the windshields or strut fairings were turned from brass. Each base section was equipped with three holes to transmit model base pressures through the hollow supporting strut to an absolute manometer for base pressure determination.

TEST PROCEDURE

The models were installed on the tunnel center line. Angles of attack from -10 to +10 degrees were covered with the tunnel at a constant supply pressure of 49 cm of Hg abs. at $M = 1.72$. Using the alternate bases, the angle of attack range from +5 to +25 degrees was covered at the same supply pressure. Lift, drag, and pitching moments were measured with the hydraulic balance system. Supply air temperature and pressure, model base pressure, and test section static pressure were also recorded. To prevent flow in the annular space between the model support strut and strut fairing, the pressure in that space was maintained equal to the model base pressure for all conditions. The supply section total pressure (P_0) was measured by a total head tube in a 64-inch diameter section upstream of the nozzle. The supply temperature (T_0) was measured by thermocouples in the supply section.

During all tests, the supply pressure was maintained at 49 cm Hg abs. giving a constant dynamic pressure of 3.61 lbs. per square inch and a constant Reynolds Number of 0.21×10^6 per inch. The characteristic length of the models was 2 inches. Throughout the test, the supply section temperature was 100°F, and the supply air specific humidity was maintained below .00020 lbs. per lb.

Schlieren photographs were taken using a parallel beam optical system having two 18" mirrors of 15' focal length.

RESULTS

The force and moment data obtained are presented in Figures 15 through 19. All data have been reduced to coefficient form using the relationships given in the Definition of Symbols. The reference length of the models was the maximum body diameter of 2.00 inches. The c.g. locations chosen for the tests are listed as follows;

<u>Model Configuration</u>	<u>Location in Calibers from the Base</u>
Caliber .50	1.466
Caliber .60	1.765
20mm	1.719

Figures 20 through 22 show the location of the center of pressure as a function of angle of attack for all configurations, calculated from wind tunnel data.

The angles of attack have been corrected for a deflection of the supporting strut under load. The change in indicated pitching moment due to strut bending was computed and was in all cases smaller than the uncertainty due to balance inaccuracies. The lift and moment curves have been translated so that they pass through the origin. This was an attempt to correct for the variation of flow inclination over the projectiles.

Previous tests have shown that the type of support used with these models can influence the model base pressure, and thus the total drag, but that, in general, the flow over the portions of the model other than the base is not affected. The effect of the strut is limited to the wake, and consequently, appears only as a change in model base pressure. Accordingly, the drag coefficient data presented in Figures 15 through 19 are obtained by subtracting from the drag coefficients, determined by the wind tunnel balance results, the base drag coefficients, determined from measurements of the model base pressure and model base area. The resultant fore drag coefficients are felt to be free of strut interference effects.

Accuracy

In general, the wind tunnel balance system can be expected to have no error greater than about three least counts. The angle of attack measurements are considered reliable to within about 0.05 degrees. The resultant uncertainties in the coefficients are as follows;

$$C_N - 0.005$$

$$C_D - 0.002$$

$$C_m - 0.026$$

DISCUSSION

Drag Data

From the data of Figures 15 through 19, the following values of the

fore drag coefficients at zero angle of attack were obtained.

Table I

<u>Configuration</u>	<u>Fore Drag Coefficient</u>
Caliber .50	.162
Caliber .50 (Rifled)	.166
Caliber .60	.180
Caliber .60 (Rifled)	.182
20mm	.270

The rifling caused an increase in the drag coefficient as might be expected.

Normal Force, Moment, and Center of Pressure

Table II shows values for $\frac{dC_N}{d\alpha}$, $\frac{dC_m}{d\alpha}$ at zero degrees angle of attack, and calculated C.P. locations.

Table II

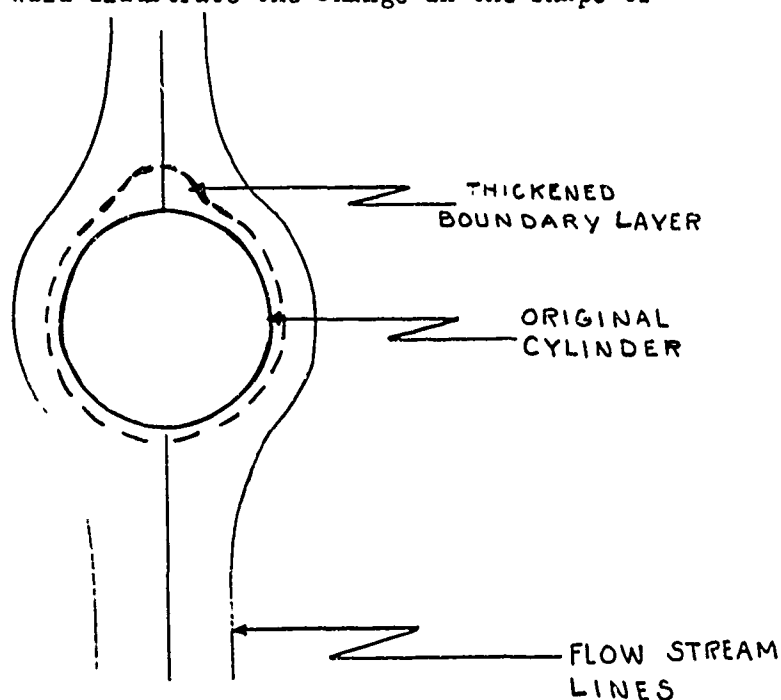
<u>Configuration</u>	$\frac{dC_N}{d\alpha}$	$\frac{dC_m}{d\alpha}$	<u>C.P. Calibers From the Base</u>
Caliber .50	.047	.070	2.96
Caliber .50 (Rifled)	.047	.073	3.02
Caliber .60	.047	.070	3.26
Caliber .60 (Rifled)	.047	.073	3.32
20mm	.047	.056	2.91

The normal force curve slope at zero angle of attack for all configurations tested was the same. Rifling produced a small change in the moment curve slope. For the assumed c.g. locations, tabulated on page 5, all configurations showed an overturning moment, which produces a destabilizing effect.

Effect of Large Angles of Attack

The data indicate that as the angle of attack is increased above

about 6 degrees, the center of pressure shifts rearward, and the normal force curve slope increases. These phenomena appear to be associated with the thickening of the boundary layer over the after body. Schlieren photographs of these projectiles show a thick boundary layer region forming first near the back of the upper surface of the body and traveling forward with increasing angle of attack, see Figures 23 through 26. As the boundary layer increased with angle of attack, the effective upper body surface was modified by the accumulation of boundary layer air. A cross-sectional view below will illustrate the change in the shape of the surface.



The center of pressure moves further aft, and the normal force curve slope increases until the angle of attack reaches about 26 degrees. In the neighborhood of 26 degrees, the variation of center of pressure and slope of normal force curve is nearly zero. These results appear in Figures 15 through 22.

Center of pressure locations in calibers from the base for $\alpha = 26^\circ$ and $\alpha = 0^\circ$ are listed on the next page.

Table III

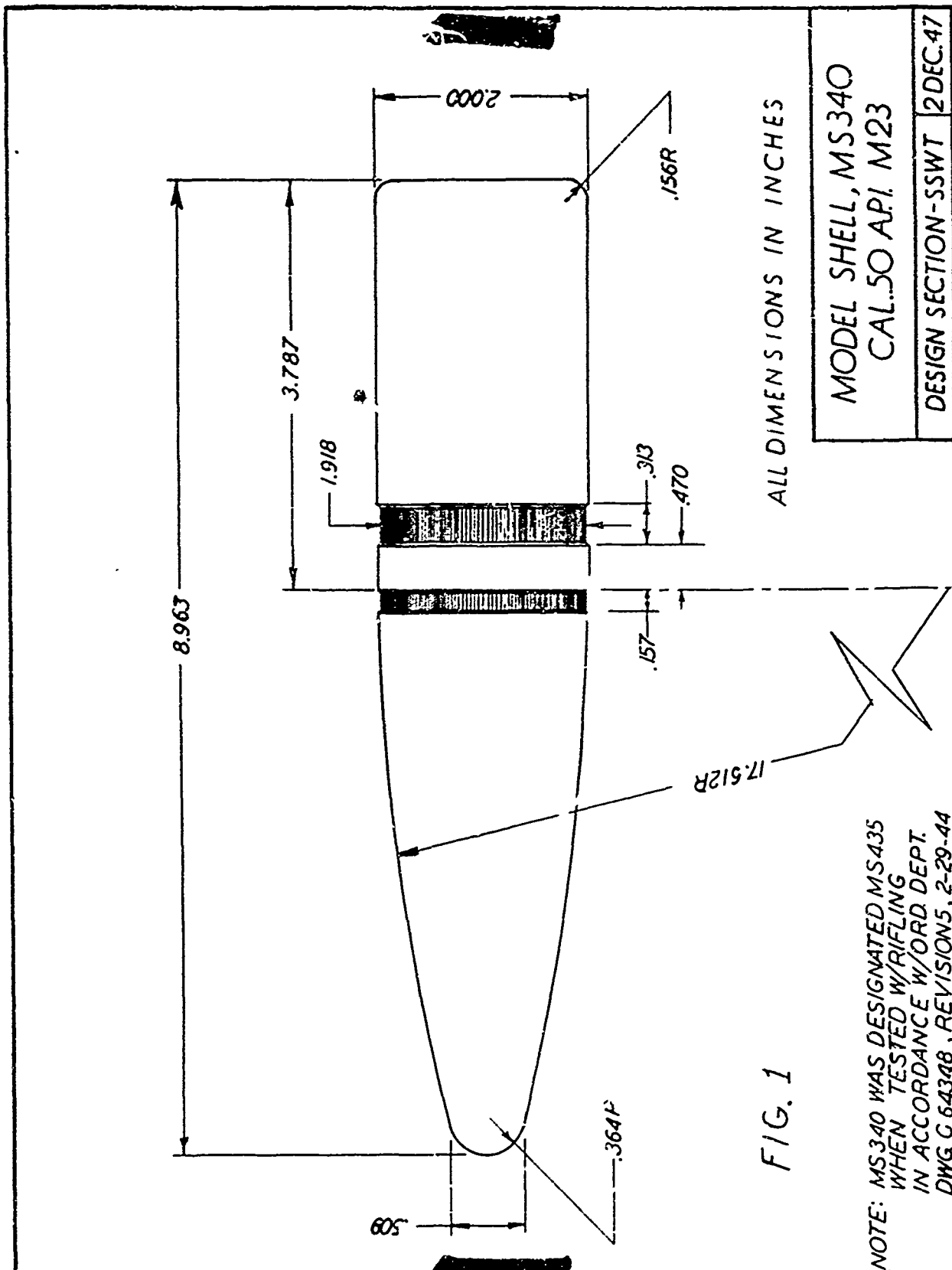
<u>Configuration</u>	<u>$\alpha = 26^\circ$</u>	<u>$\alpha = 0^\circ$</u>
	<u>C.P. Location in Calibers From Base</u>	<u>C.P. Location in Calibers From Base</u>
Caliber .50	2.28	2.96
Caliber .50 (Rifled)	2.35	3.02
Caliber .60	2.40	3.26
Caliber .60 (Rifled)	2.45	3.32
20mm	2.19	2.91

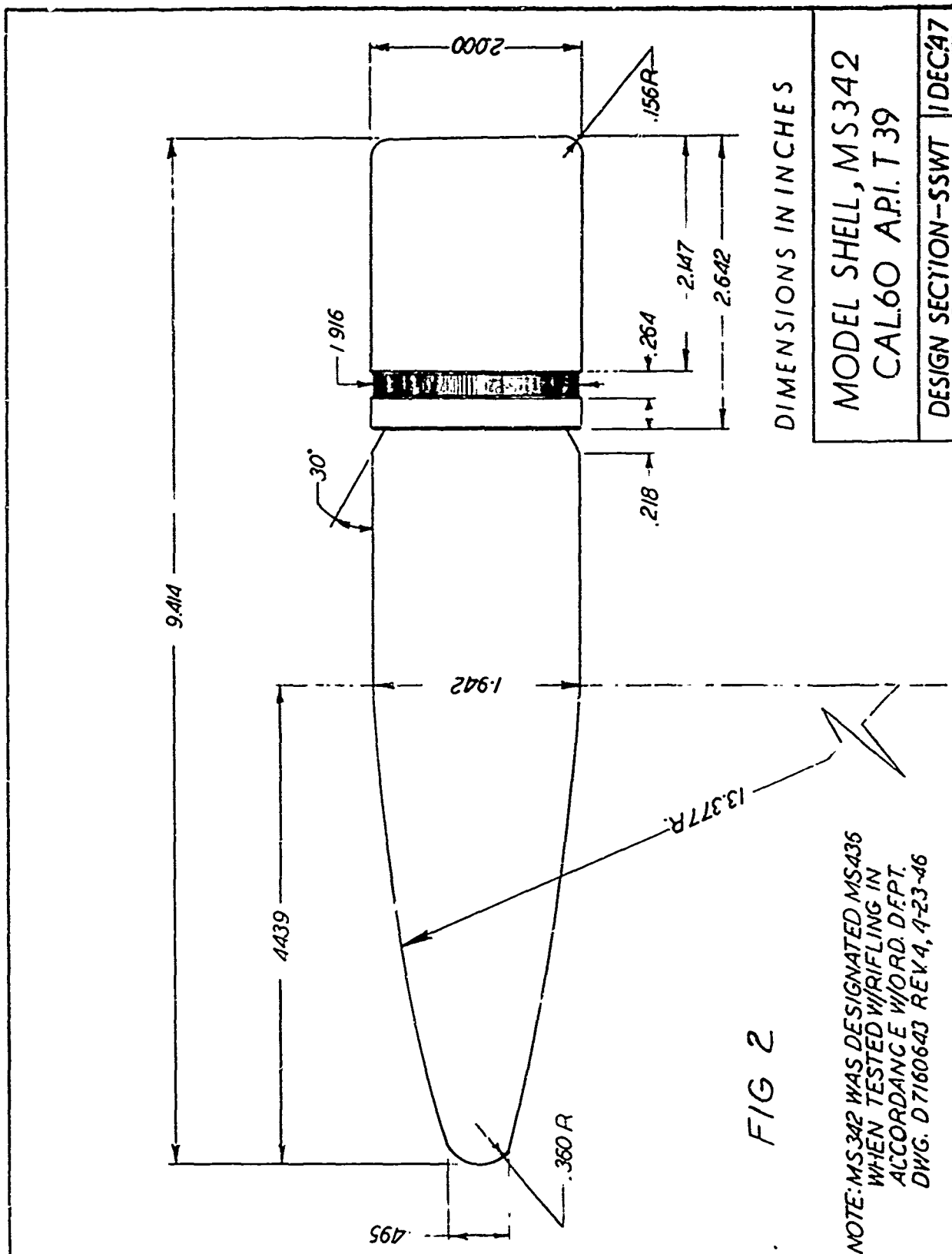
CONCLUSIONS

The entire group of small projectiles tested were found to be aerodynamically unstable.

The addition of rifling on the Caliber .50 and .60 projectiles produced an increase in the fore drag coefficient and slightly increased the moment curve slope.

At large angles of attack, a rearward travel of the center of pressure, and an increase in the slope of the normal force curve were observed. These effects were apparently due to the increasing thickness of the boundary layer over the upper surface of the after body.





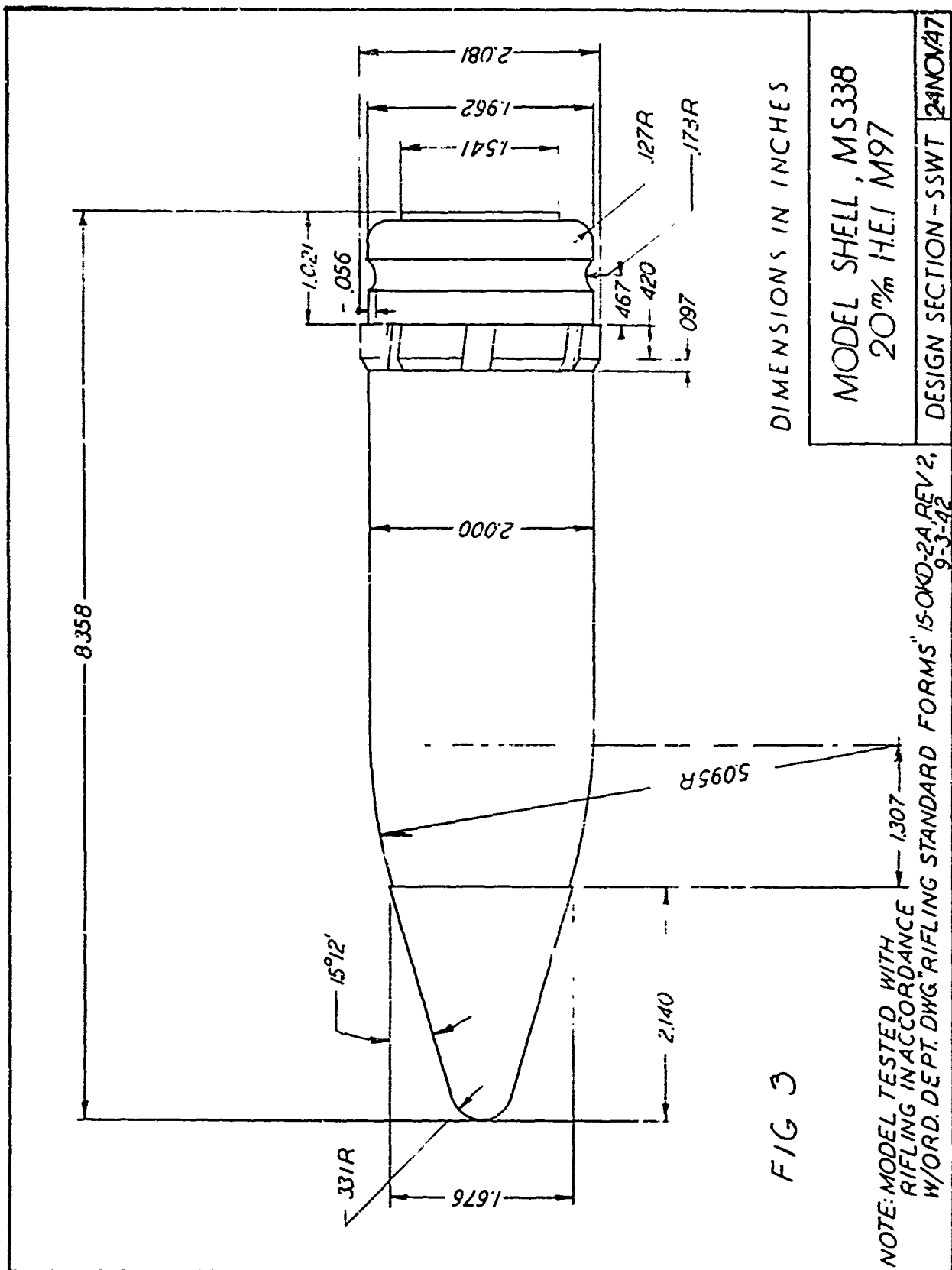
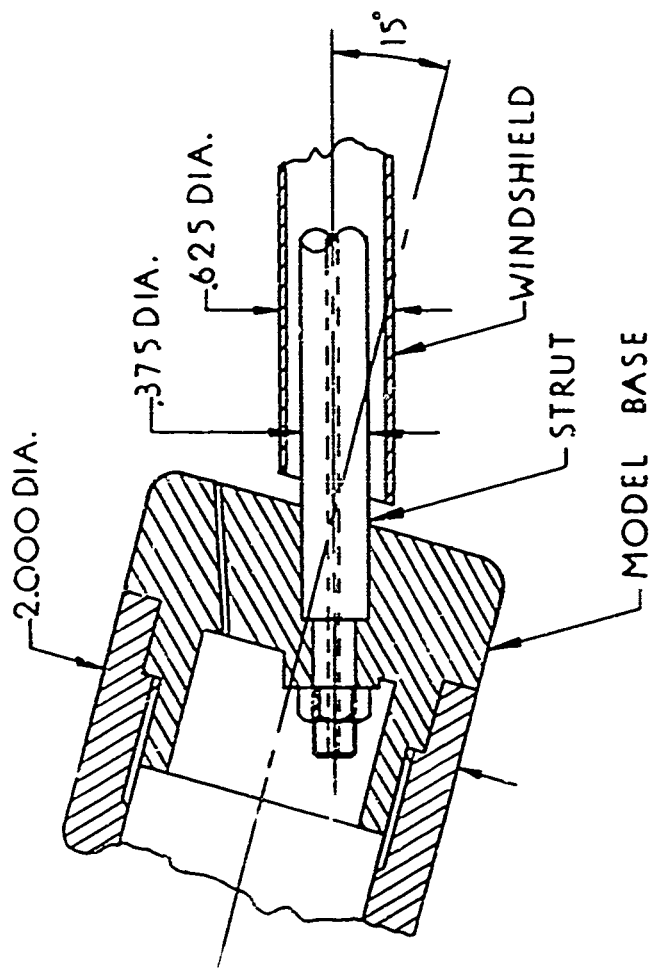


FIG 3



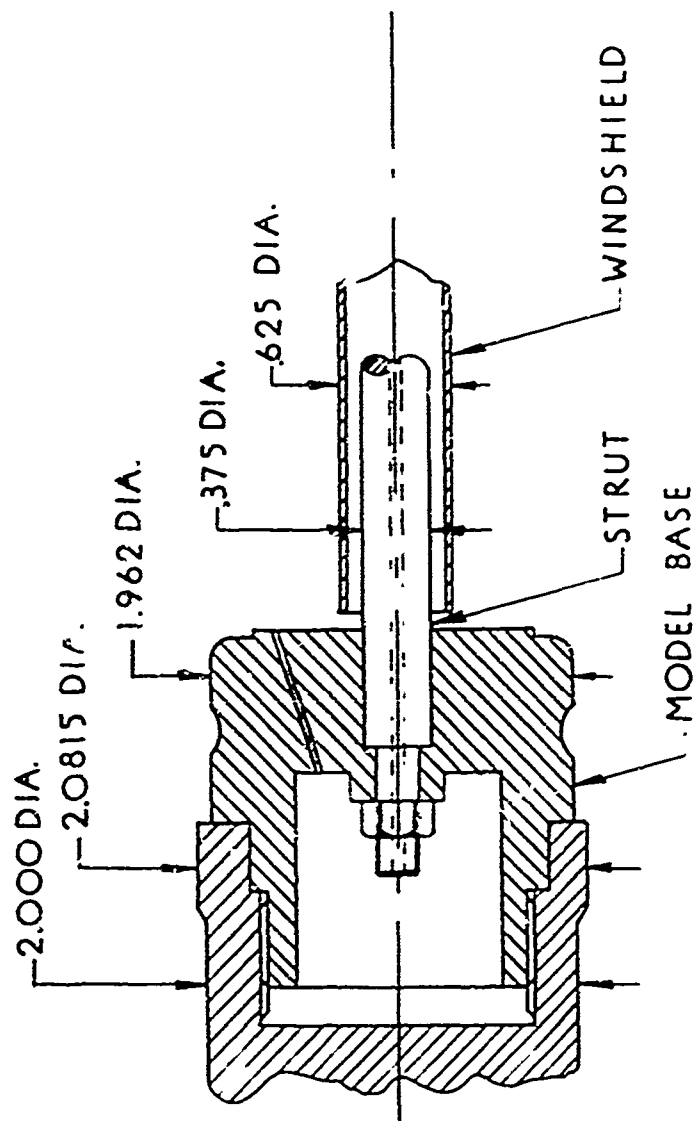
TYPICAL SECTION VIEW OF SPECIAL SUPPORT FOR .50 & .60 CAL. PROJECTILES

FIG 4

DIMENSIONS IN INCHES

MS341, MS343
MS434, MS437

SUPERSONIC WIND TUNNELS SEPT. '48



TYPICAL SECTION VIEW
OF STRAIGHT SUPPORT
FOR 20MM PROJECTILE

FIG 5

DIMENSIONS IN INCHES

MS338 & MS339

SUPERSONIC WIND TUNNELS SEPT. '48

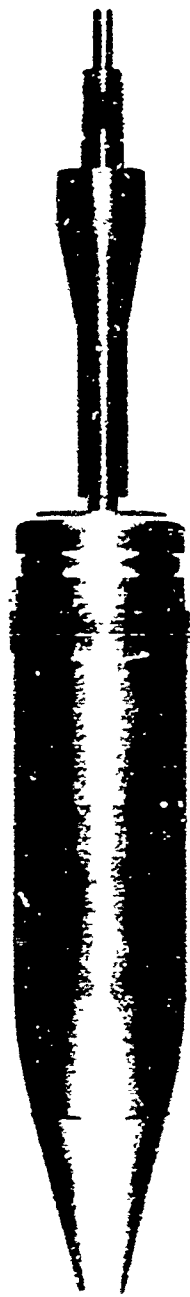


FIGURE 6. MS 338, 30mm Projectile, Wind Tunnel Model.



FIGURE 7. MS 339, 20mm Projectile, Wind Tunnel Model.



FIGURE 8. MS 340, Cal. .50 Projectile, Wind Tunnel Model.



FIGURE 9. MS 435, Cal. .50 Projectile (rifled), Wind Tunnel Model.



MS 341

FIGURE 10. MS 341, Cal. .50 Projectile, Wind Tunnel Model.



FIGURE 11. MS 342, Cal. .60 Projectile, Wind Tunnel Model.



FIGURE 12. MS 436, Cal. .60 Projectile (Rifled), Wind Tunnel Model.

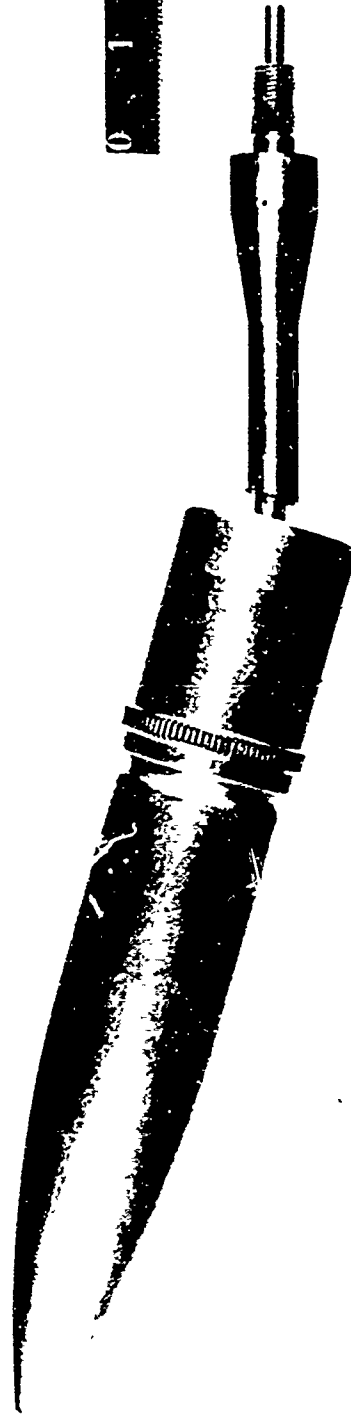


FIGURE 13. MS 343, Cal. .60 Projectile, Wind Tunnel Model.

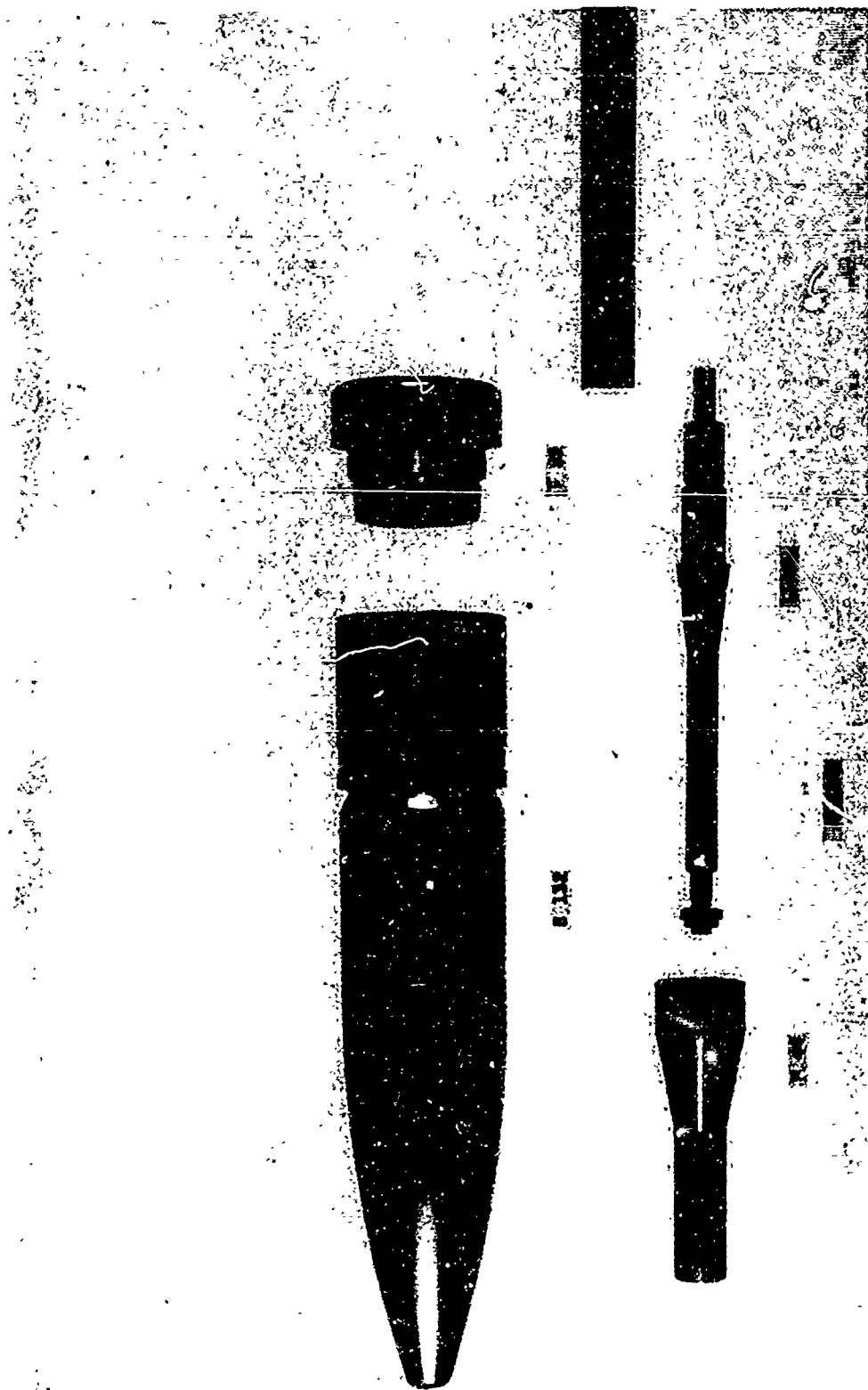
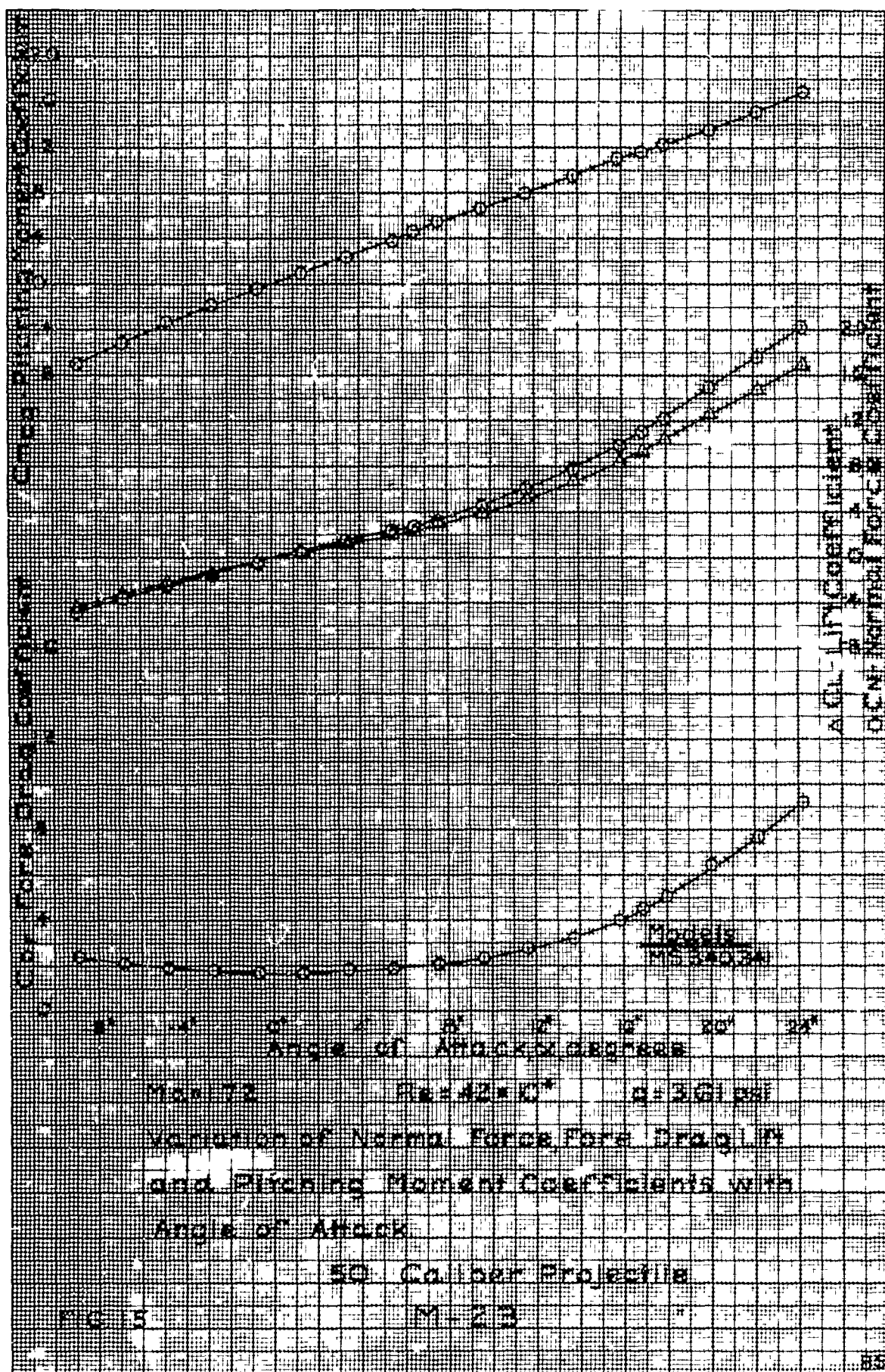
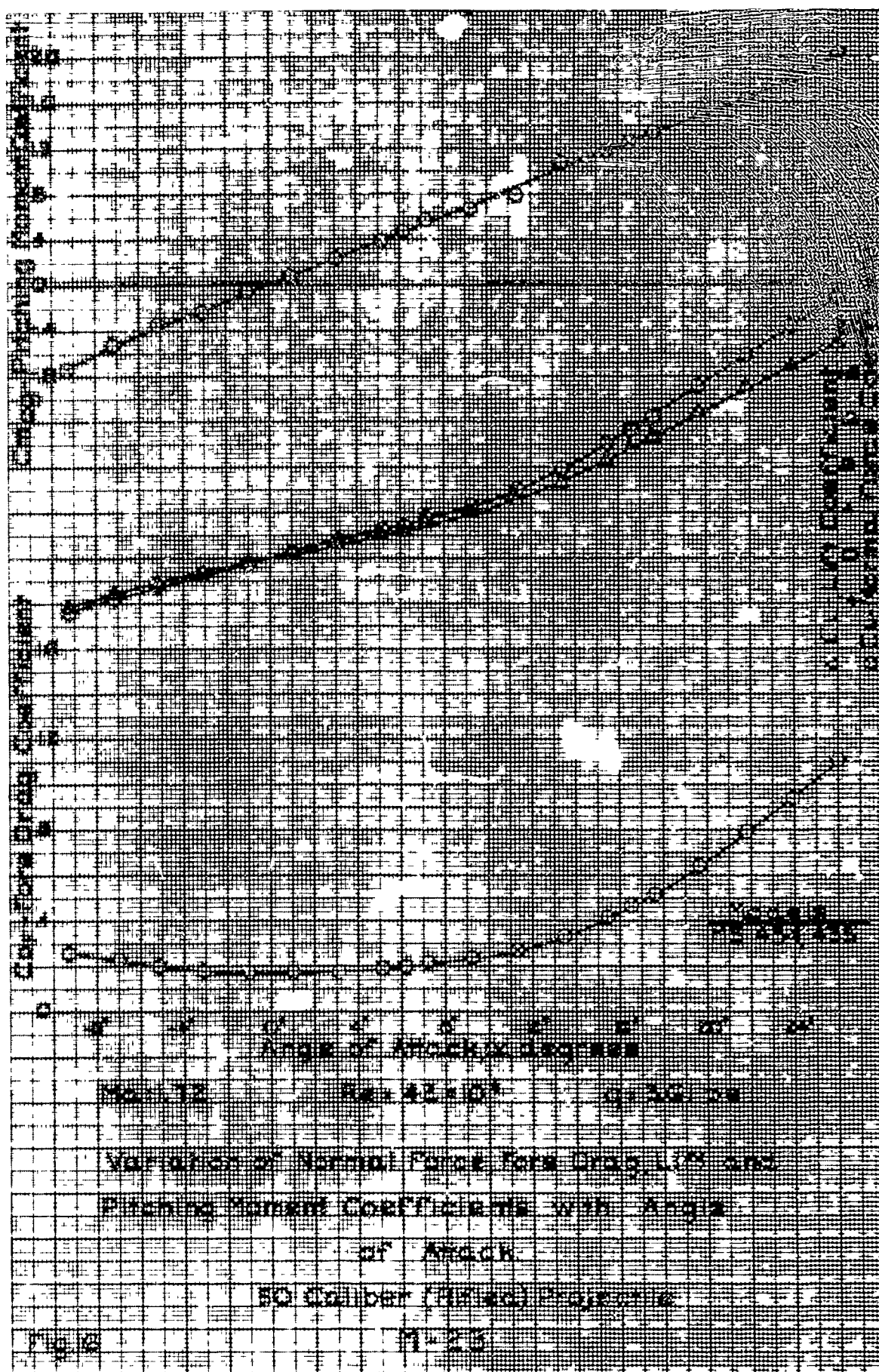
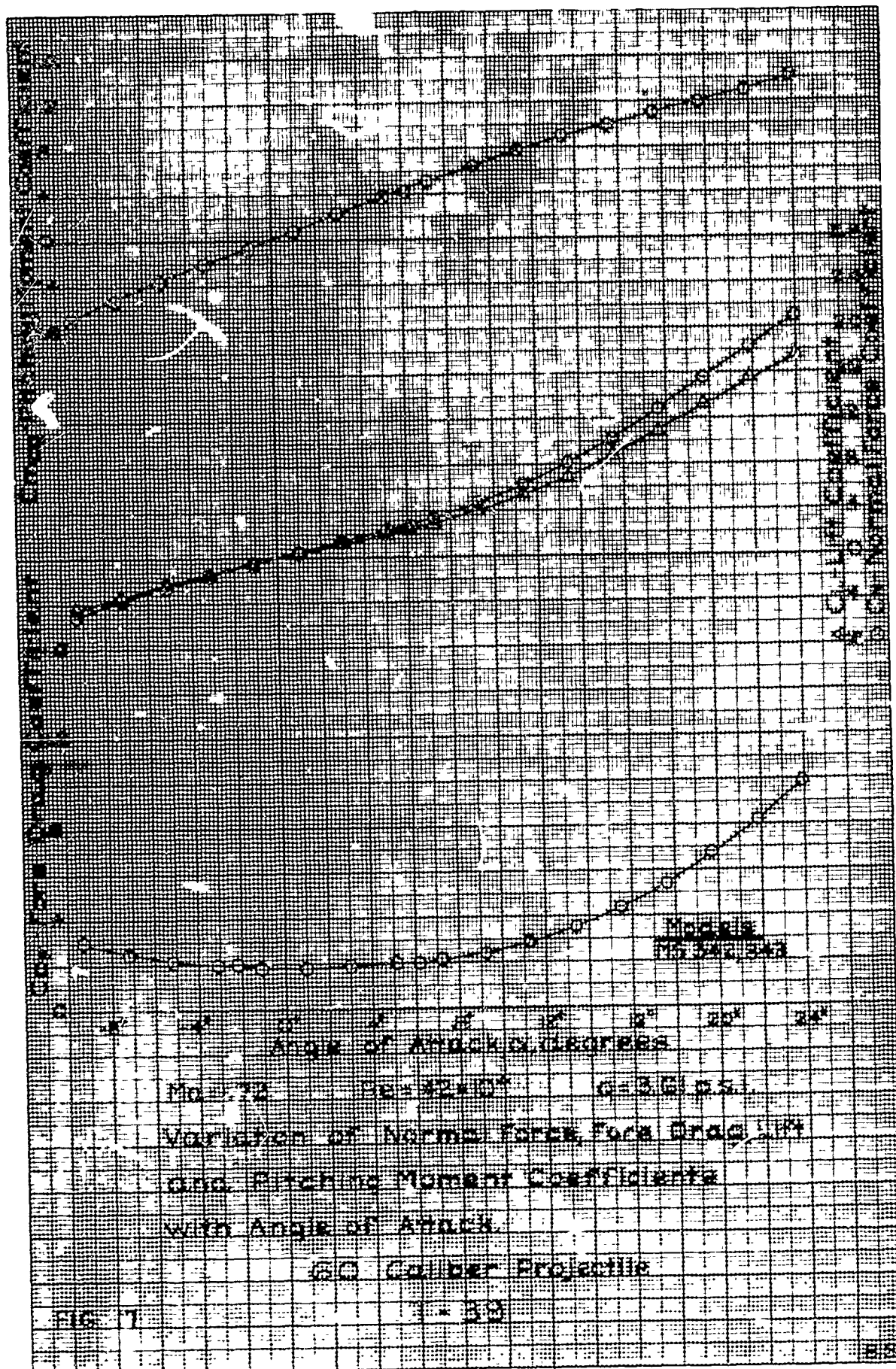
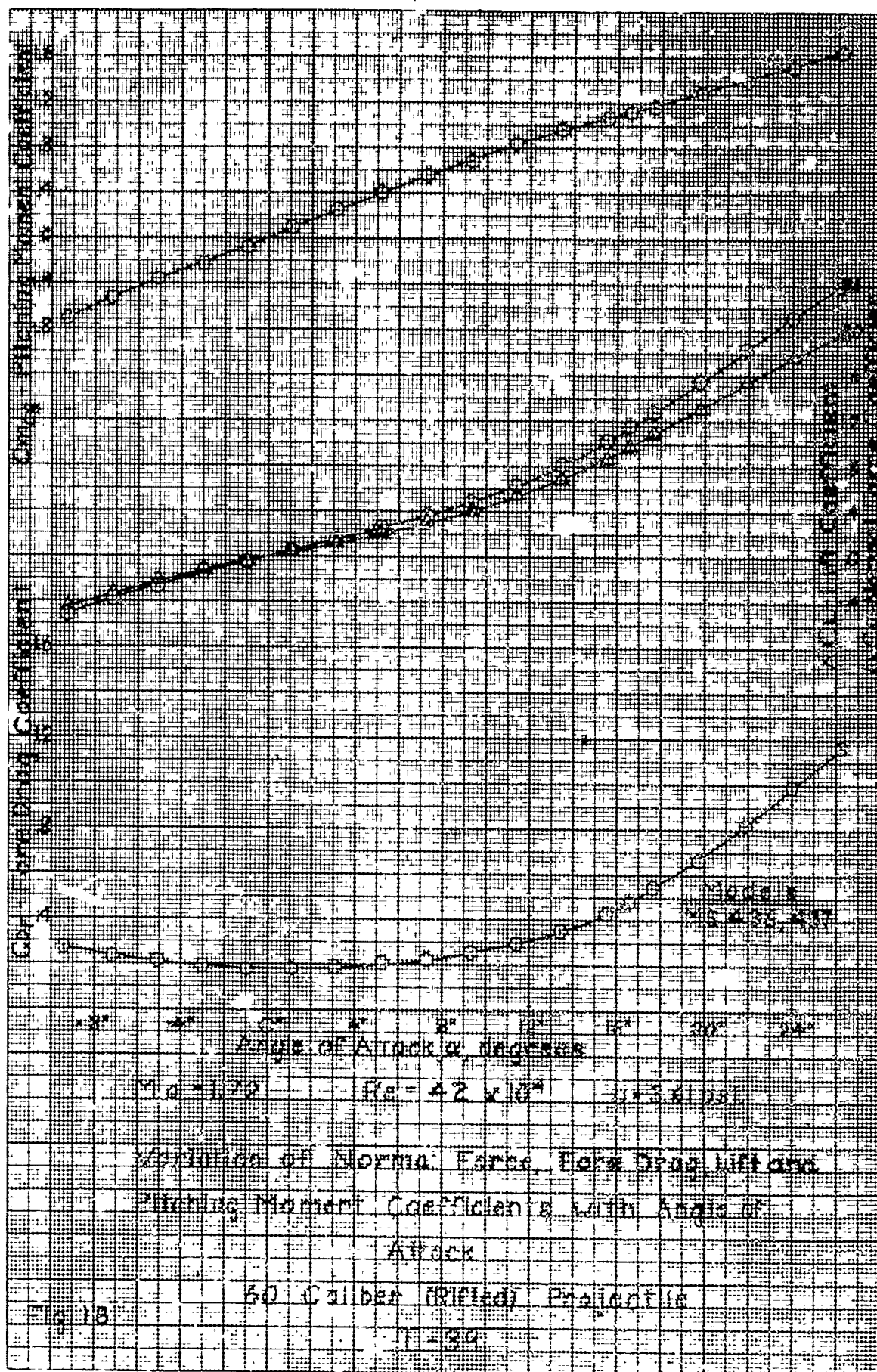


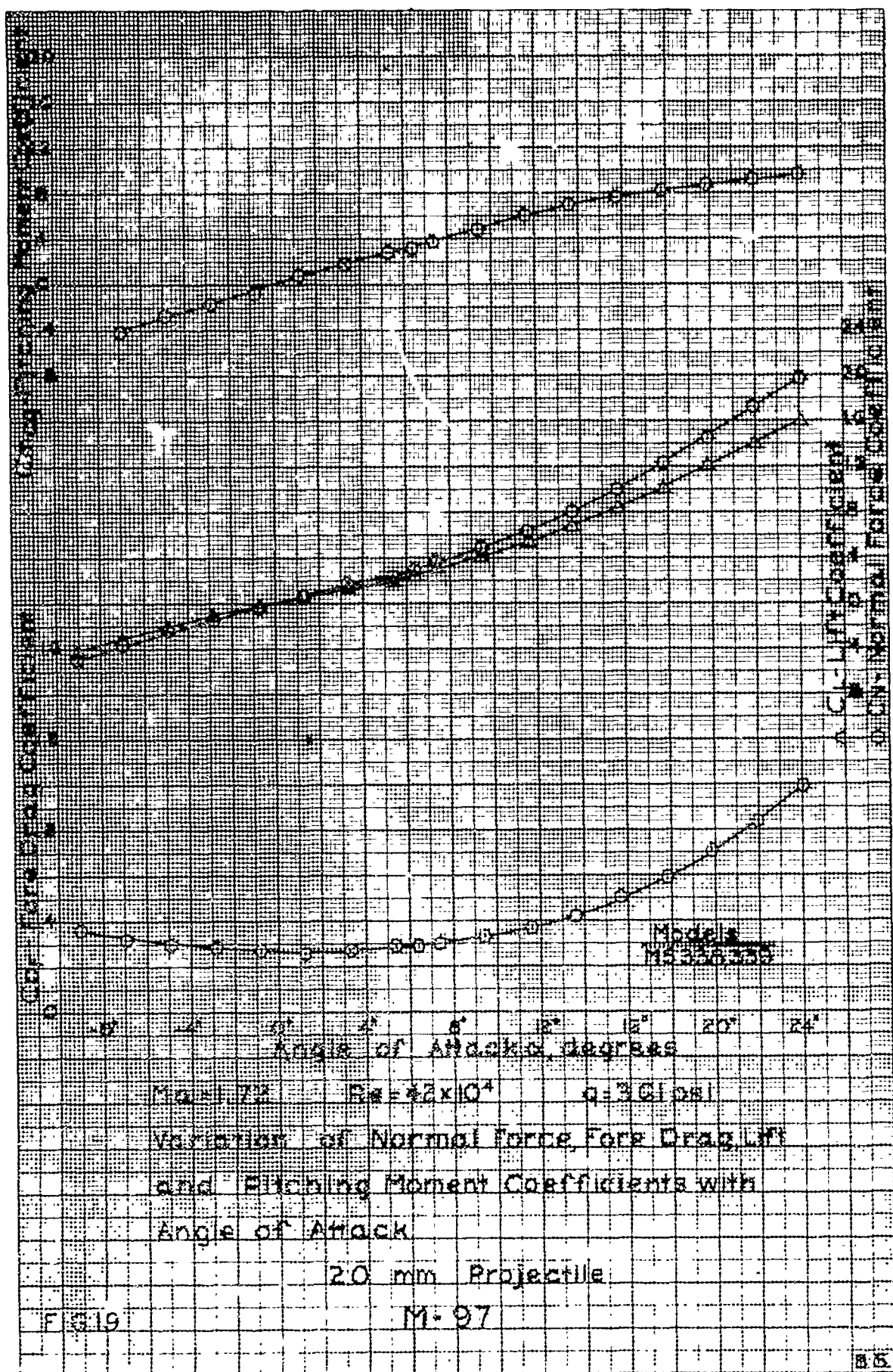
FIGURE 14. MS S42, Cal. .60 Projectile Components, Wind Tunnel Model.

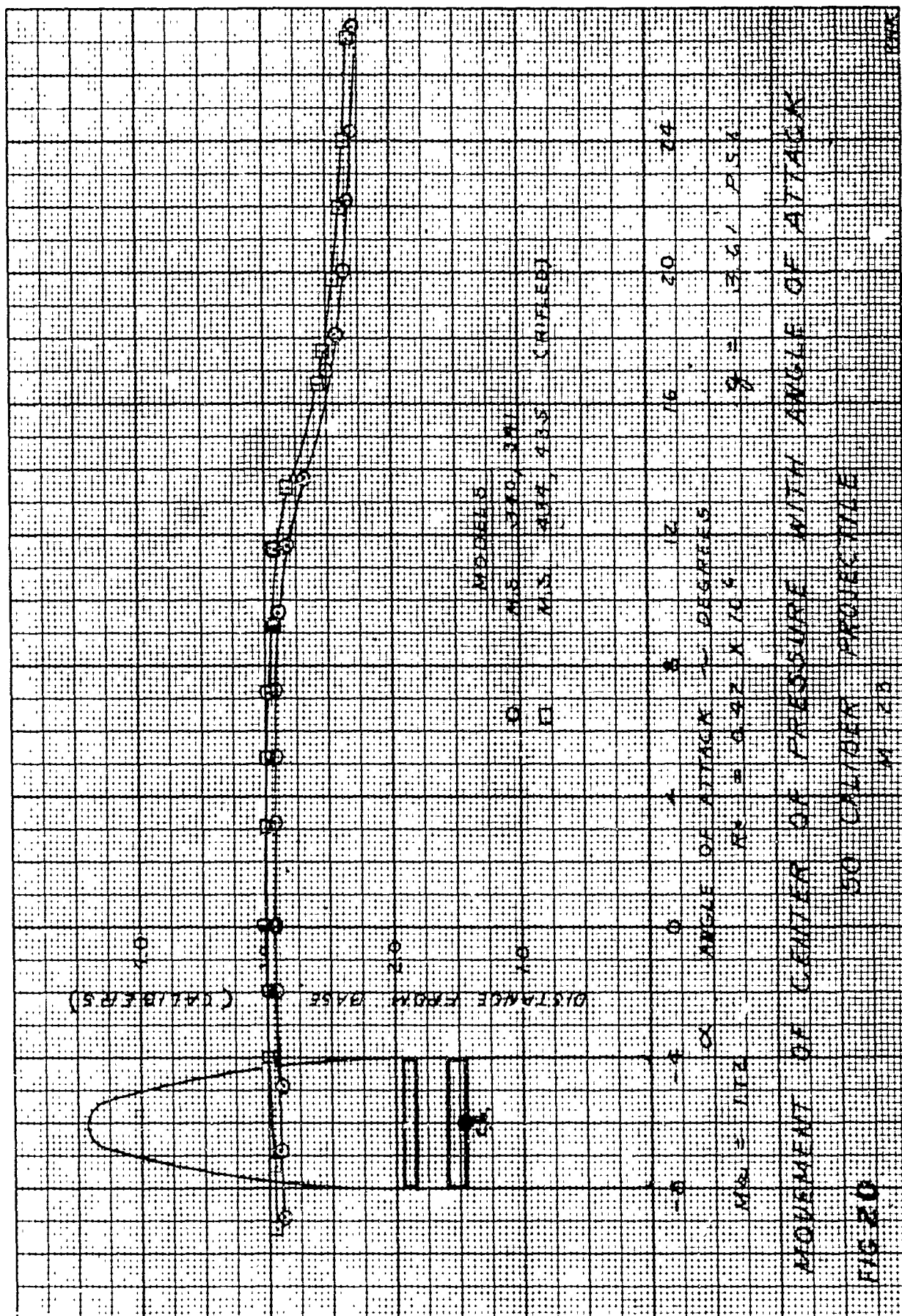


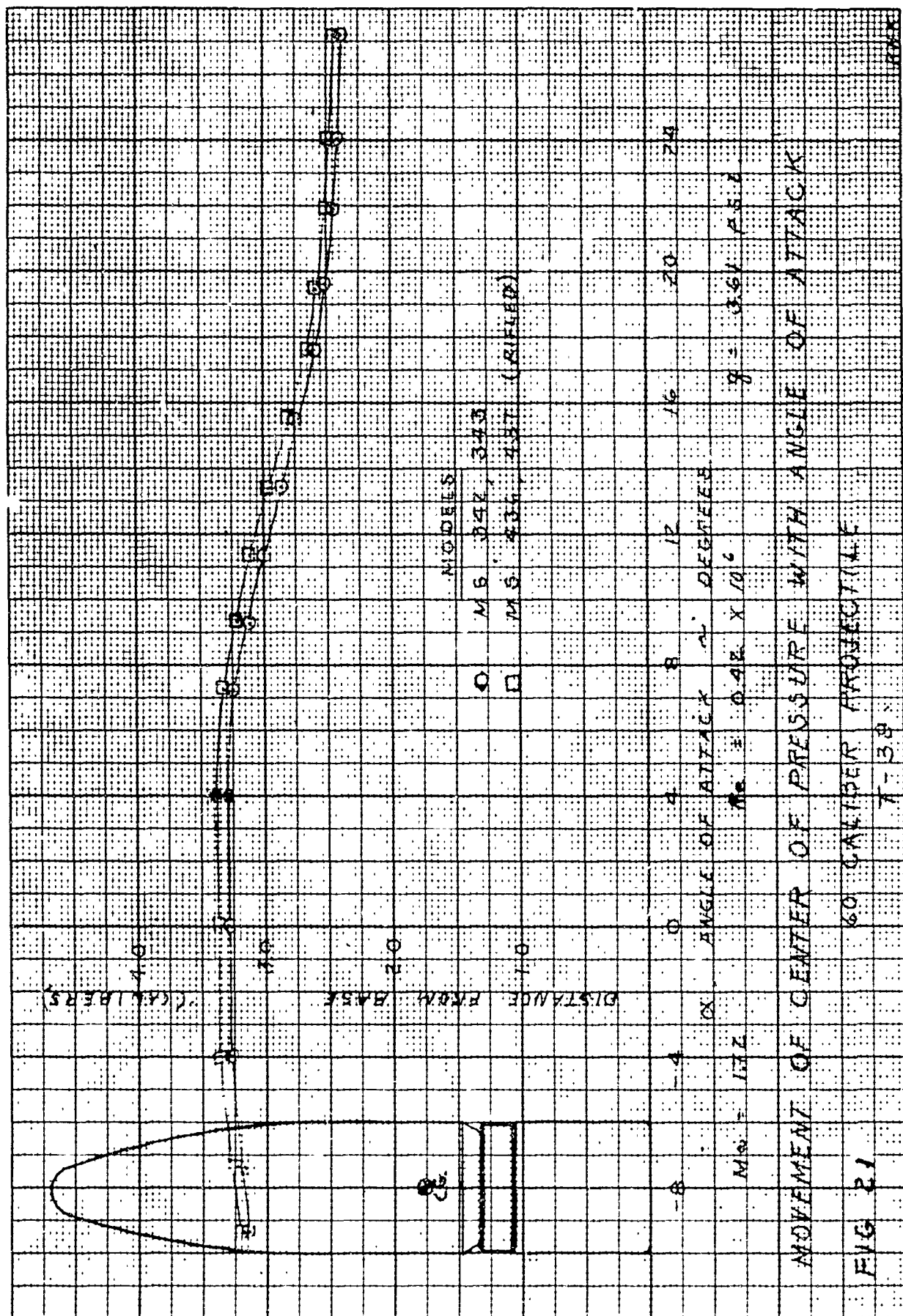


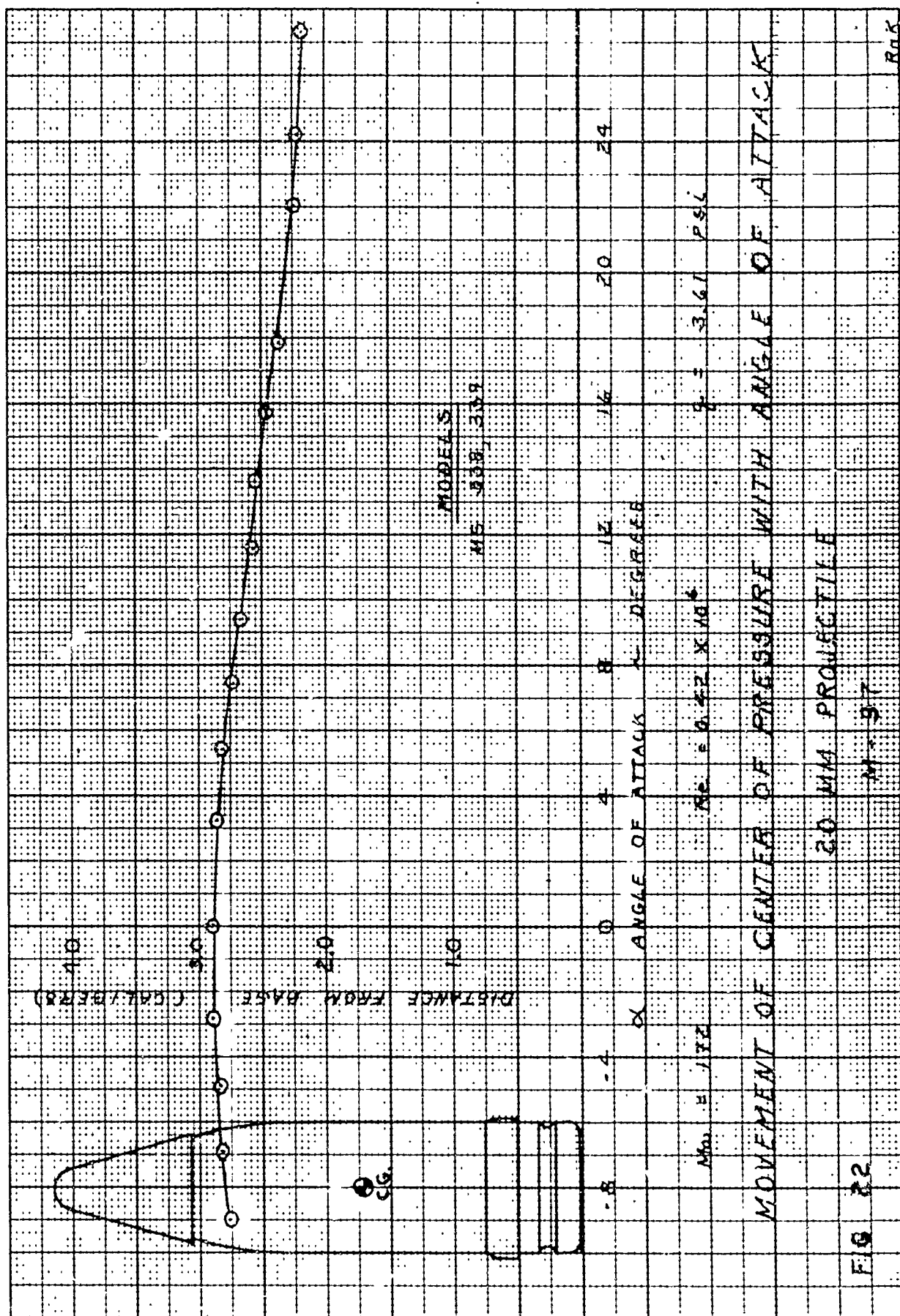












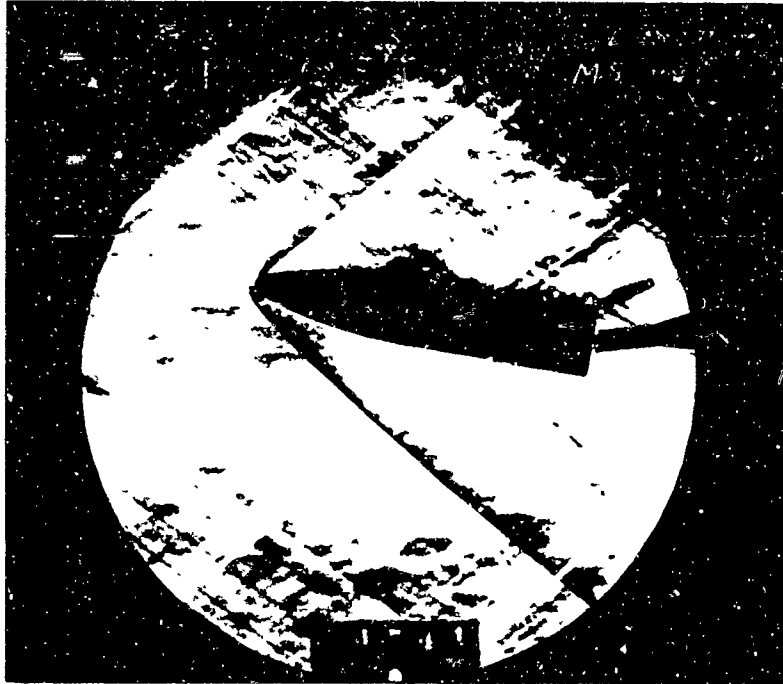


FIGURE 23 Schlieren photograph of the Caliber .60 (rifled) projectile model at $\alpha = +10^\circ$ to centerline of flow. The offset strut is used.



FIGURE 24 Schlieren photograph of the Caliber .60 (rifled) projectile model at $\alpha = +25^\circ$ to centerline of flow. The offset strut is used.



FIGURE 25. Schlieren photograph of the Caliber .50 (rifled) projectile model at $\alpha = +5^\circ$ to centerline of flow. The offset strut is used.

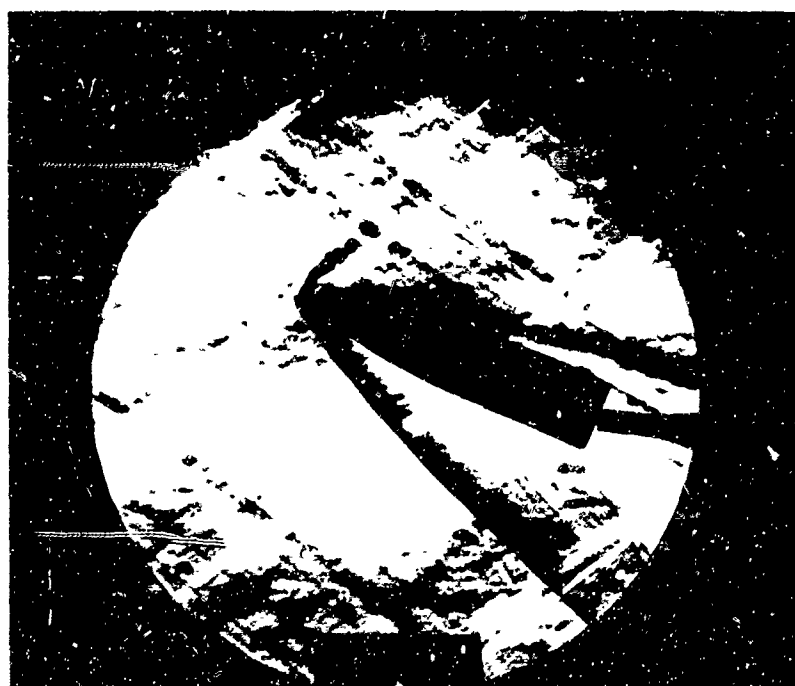
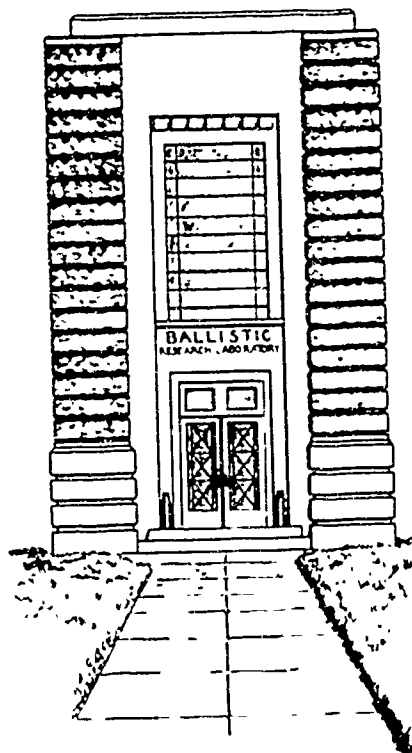


FIGURE 26. Schlieren photograph of the Caliber .50 (rifled) projectile model at $\alpha = 22^\circ$ to centerline of flow. The offset strut is used.



DUPLICATING BRANCH
THE ORDNANCE SCHOOL
ABERDEEN PROVING GROUND
MARYLAND